Supporting Information

Influence of Functional Groups on Organic Aerosol Cloud Condensation Nuclei Activity

Sarah R. Suda[1], Markus D. Petters[1], Geoffrey K. Yeh[2+], Christen Strollo[2,†], Aiko Matsunaga[2,‡], Annelise Faulhaber[2], Paul J. Ziemann[2,§], Anthony J. Prenni[3,ǀ], Christian M. Carrico[3,¶], Ryan C. Sullivan[3,#], and Sonia M. Kreidenweis[3]*

[1]North Carolina State University, Dept. of Marine Earth and Atmospheric Sciences, Raleigh, NC, USA
[2]University of California Riverside, Air Pollution Research Center, Riverside, CA, USA
[3]Colorado State University, Department of Atmospheric Science, Fort Collins, CO, USA

[+]now at Peal Therapeutics, 200 Saginaw Drive, Redwood City, CA, 94063-4725
[†]now at College of St. Benedict and St. John's University, Dept. of Chemistry, St. Joseph, MN, USA
[‡]now at California Air Resources Board, Emission Compliance, Automotive Regulations and Sciences Division, El Monte, CA, USA
[§]now at University of Colorado, Department of Chemistry and Biochemistry, Boulder, CO, USA
[ǀ]now at National Park Service, Air Resources Division, Lakewood, CO, USA
[¶]now at New Mexico Inst. of Mining and Technol., Dept. of Civil and Environ. Eng., Socorro, NM, USA
[#]now at Carnegie Mellon University, Center for Atmospheric Particle Studies, Pittsburgh, PA, USA

Corresponding Author
*Markus D. Petters (markus_petters@ncsu.edu), Dept. of Marine Earth and Atmospheric Sciences, Campus Box 8208, Raleigh, NC 27695, USA

This PDF includes 14 pages:

Relationship between O:C ratio and κ for pure compounds; O:C ratio as seen by the Aerosol Mass Spectrometer; Molecule structure identification; Figure S1, S2; Scheme S1; Tables S1–S5; References

Relationship between O:C ratio and κ for pure compounds

Jimenez et al.[1] report tight correlations between the atomic O:C ratio and κ for a number of complex OA observed in field studies of hygroscopic growth. These observed strong relationships between a simple proxy for composition, such as the atomic O:C ratio, and κ are not predicted by the behavior of pure compounds, as shown in Figure S1. The pure compounds studies, however, suggest that $\kappa \sim 0$ for O:C < 0.2, in accordance with field observations.

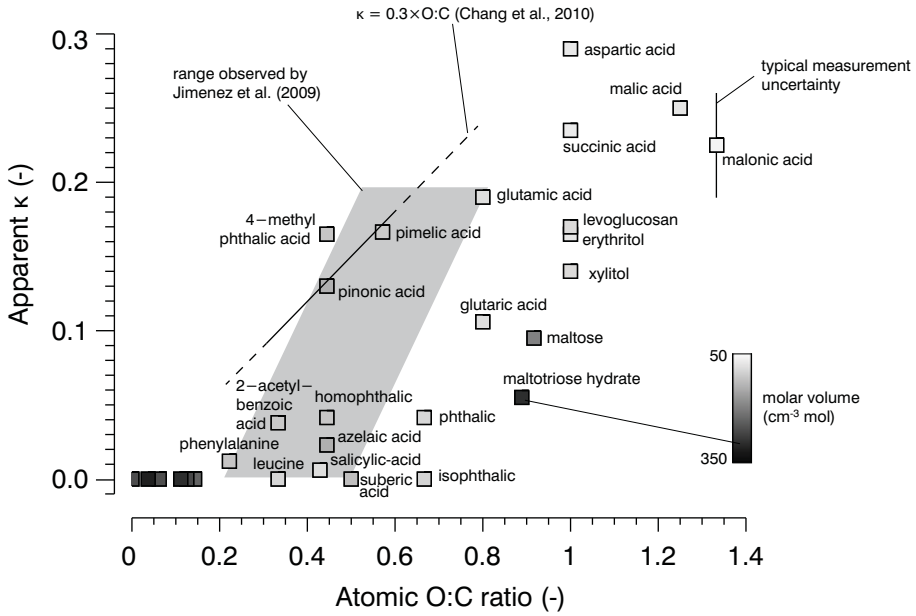

Figure S1. CCN derived κ values for individual compounds listed in the supporting information of Petters et al.[2] graphed vs. their atomic O:C ratio. Grey shading within the symbol indicates the molar volume of the compound. Grey trapezoid indicates the range and slope of the relationship observed by Jimenez et al.[1] Dashed line shows the extrapolated relationship of the study by Chang et al.,[3] strictly valid between 0.3 < O:C < 0.6.

O:C ratio as seen by the Aerosol Mass Spectrometer

Many studies use Aerosol Mass Spectrometer (AMS) data to report the O:C ratio of organic aerosols. However, the AMS most likely under-observes the O:C from organic nitrates[4] such that ONO_2 moieties are interpreted as NO and the NO_2 fragment is misattributed as inorganic nitrate. In Figure S2 we adjust the data from Figure 3 to simulate this artifact and facilitate comparison to studies using AMS-derived O:C ratios.

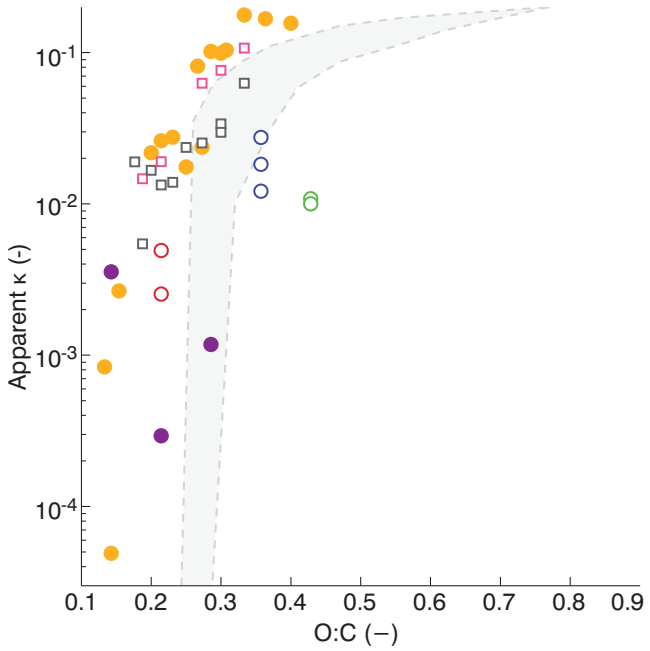

Figure S2. Kappa plotted against the O:C ratio from molecular formulas. This figure is an adjustment to Figure 3 with nitrate groups contributing only one oxygen to the organic O:C ratio, as expected for studies using the Aerosol Mass Spectrometer.[4] Colors indicate the functional group targeted. Gold: hydroxyl (-OH), Fig. 2A; blue: carboxylic acid (-C(=O)OH), Fig. 2B; green: hydroperoxide-ether (-C(OOH)-O-), Fig. 2C; purple: nitrate ($-ONO_2$), Fig. 2D; black and pink: methylene ($-CH_2-$) groups, Fig. 2E. Open symbols correspond to hydroperoxides (circle = liquid synthesis, square = chamber reaction). Filled symbols correspond to hydroxynitrates. The shaded region traces out the data reported by Jimenez et al.[1]

Molecule structure identification

(1) Hydroperoxide experiments (Scheme 1; Figure 2B, C; Table S1)

Hydroperoxides synthesized in liquid ozonolysis formed at near 100% yield.[5,6] After the reaction was completed, the synthesized mixture was passed through the HPLC coupled with the thermal desorption mass spectrometer. The retention time was recorded and the presence of one or two ion mass fragments expected from the product was confirmed for each of the species shown in Figure 2 panels B and C.

For the *x,y* ozonolysis reaction, *x* is carbon number of the alkene and *y* is the carbon number of the alcohol. The product carbon number is C_{x-1+y} for the reaction 1-alkenes or 1-alkenoic acids with O_3 in the presence of alcohol, and C_{x-2+2y} for the reaction of 1,n-dienes with O_3 in the presence of alcohol.

(2) Hydroperoxide experiments (Figure 2 panel E; Table S3)

Hydroperoxide aerosol formed in the gas-phase reaction consists of multiple products. For the *x,y* reaction, the main compound expected in the condensed phase is the C_{x-1+y} α-alkoxy-hydroperoxide (the proposed structure shown in Figure 2E) with minor fractions of $C_{2(x-1+y)}$ secondary ozonide, and the $C_{2(x-1+y)}$ peroxyhemiacetal present.[7,8] The number of CH_2 groups in the molecule is x+y-4.

(3) Hydroxynitrate experiments (Figure 1; Figure 2A, D; Scheme S1; Table S2)

β-hydroxynitrates, dihydroxynitrates, and trihydroxynitrates comprise the three main products from the reaction of 2-methyl-1-alkenes with OH in the presence of NO_x.[9] The reaction mechanism is provided in Scheme S1, and the generation of C_{14} di-, tri- and tetranitrates according to the method of Kames et al.[10] is described in the main text. These products are

clearly separable in the HPLC-UV chromatogram and mapping between peak retention time and molecular structure is obtained by HPLC coupled with thermal desorption mass spectrometry (cf. Figure 2 by Matsunaga and Ziemann).[9] For the 2-methyl-1-tetradecene reaction the retention times for the β-hydroxynitrates, dihydroxynitrates, and trihydroxynitrates are 50, 30, and 7 min, respectively. Di- and trihydroxynitrate isomers did not separate in the HPLC. Retention times shift slightly for different precursor carbon numbers. Using the identical gradient elution method allowed compound identification via retention time alone.

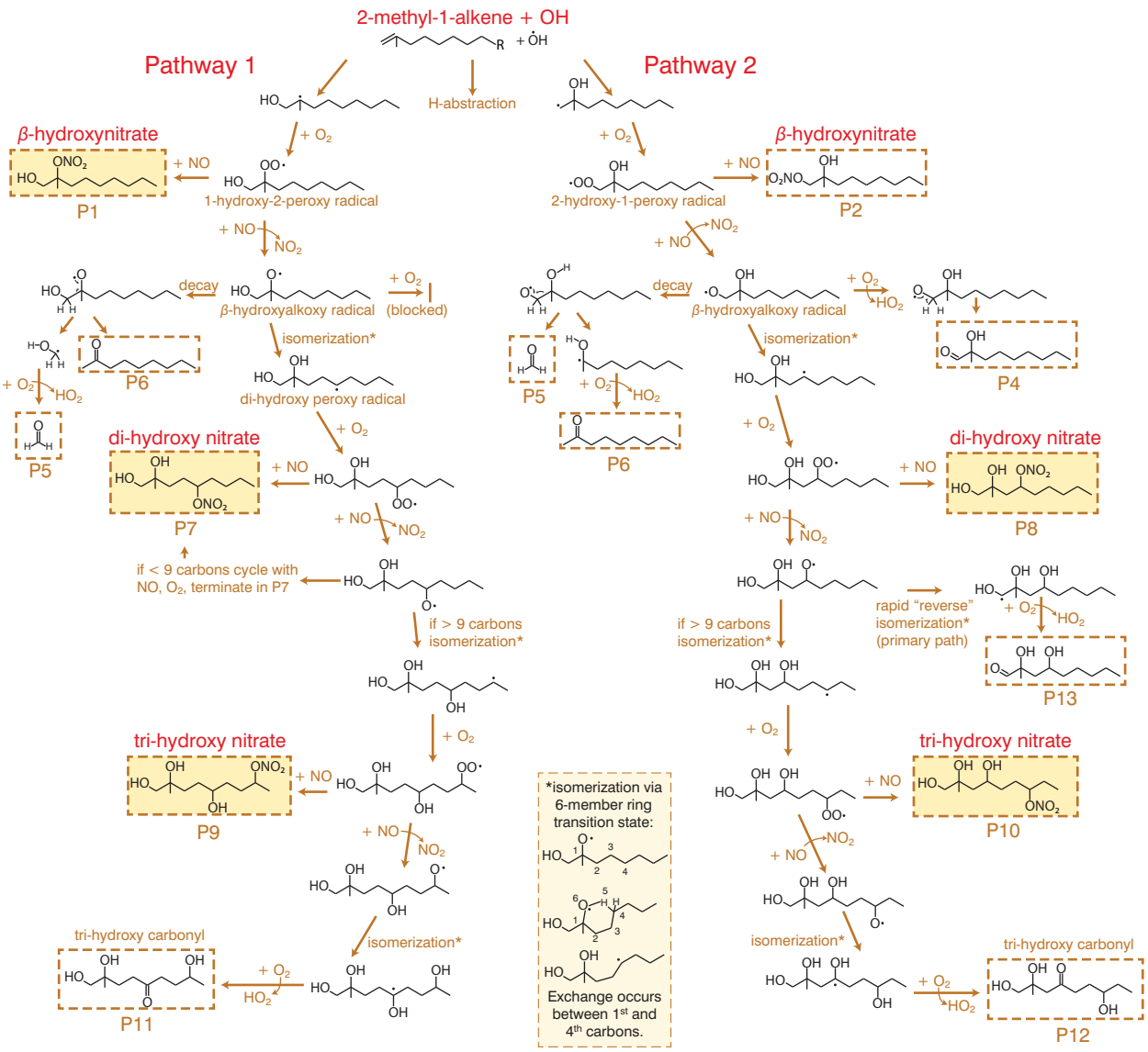

Scheme S1. Mechanism of hydroxynitrate generation in gas phase environmental chamber reactions from C_{10}–C_{15} 2-methyl-1-alkenes based Figure 1 by Matsunaga and Ziemann.[9] Note that Pathways 1 and 2 are symmetric, producing isomers. Differences occur at juncture 2, where the "+ O_2" path is only available to Pathway 2, and at juncture 4, where the "reverse isomerization" is only available to Pathway 2. Separation by HPLC gives three peaks: trihydroxynitrate isomers (P9 + P10), dihydroxynitrate isomers (P7 + P8), and 1-hydroxy-2-nitrooxy-2-methylalkane (β-hydroxynitrate isomer P1).[9]

Supplementary tables

Table S1. Averaged κ values and standard deviation of κ for C_{14} molecules synthesized by liquid ozonolysis of 1-alkenes, alkenoic acids and dienes in the presence of excess alcohol.[5,6] κ was obtained by HPLC-CCN analysis.[8] Column 1 is an experiment identifier corresponding to Figure 2 panels B and C, column 2 contains the reactants, columns 6–7 are the number of hydroperoxide-ether (-C(OOH)-O-) and carboxyl (-C(=O)OH) groups per product molecule, and columns 8–10 are the data from repeated HPLC injections of the same sample.

Molecule Number	Alkene, Alcohol	Product structure	κ [-]	stdev [-]	C(OOH) -O-	C(=O)OH	Dd [nm]	s_c [%]	κ [-]
1	1-dodecene, propanol	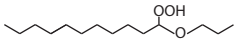	2.53×10^{-3}	9.02×10^{-4}	1	0	142	0.52	1.60×10^{-3}
							205	0.59	2.60×10^{-3}
							278	0.37	3.40×10^{-3}
2	1-tridecene, ethanol	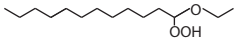	4.91×10^{-3}	5.87×10^{-3}	1	0	140	0.59	1.24×10^{-3}
							177	0.53	6.77×10^{-3}
							222	0.74	4.48×10^{-4}
							264	0.87	$< 1\times10^{-5}$
3	6-heptenoic acid, 1-octanol	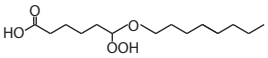	2.75×10^{-2}	1.27×10^{-2}	1	1	142	0.34	3.96×10^{-2}
							205	0.23	2.84×10^{-2}
							243	0.26	1.43×10^{-2}
4	9-decenoic acid, 1-pentanol	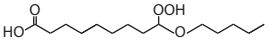	1.82×10^{-2}	7.39×10^{-3}	1	1	120	0.62	1.87×10^{-2}
							142	0.42	2.53×10^{-2}
							243	0.29	1.06×10^{-2}
5	10-undecylenic acid, 1-butanol	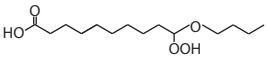	1.21×10^{-2}	5.37×10^{-3}	2	0	205	0.31	1.59×10^{-2}
							209	0.29	1.75×10^{-2}
							243	0.33	7.54×10^{-3}
							278	0.27	7.43×10^{-3}
6	1,9-decadiene, 1-propanol	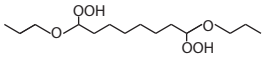	9.97×10^{-3}	2.62×10^{-3}	2	0	103	0.99	9.11×10^{-3}
							123	0.76	9.67×10^{-3}
							123	0.83	7.47×10^{-3}
							223	0.30	1.36×10^{-2}
7	1,7-octadiene, 1-butanol	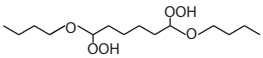	1.08×10^{-2}	4.20×10^{-3}	2	0	205	0.31	1.64×10^{-2}
							209	0.35	1.14×10^{-2}
							243	0.31	8.85×10^{-3}
							278	0.29	6.58×10^{-3}

Table S2. Averaged κ values and standard deviation of κ for hydroxynitrates generated in gas phase reactions.[9] κ was obtained by HPLC-CCN analysis.[8] Column 1 is an experiment identifier corresponding to Figure 2 panels A and D. Structures in column 3 (Molecules 8–22) correspond to Scheme S1 products P1 (β-hydroxynitrates), P8 (dihydroxynitrates), and P10 (trihydroxynitrates). Generation of molecules 23–25 is described in the main text. Column 6 is the product carbon chain length, columns 7–8 are the number of hydroxyl (-OH) and nitrate (-ONO_2) groups per product molecule and columns 9–11 are the data from repeated HPLC injections of the same sample.

Molecule Number	Name	Product structure	κ [-]	stdev [-]	C	OH	ONO_2	D_d [nm]	s_c [%]	κ [-]
8	C_{10} dihydroxy-nitrate	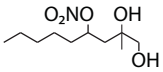	9.88×10^{-2}	6.37×10^{-2}	10	2	1	82	0.38	1.69×10^{-1}
								103	0.37	9.25×10^{-2}
								103	0.32	1.18×10^{-1}
								177	0.39	1.59×10^{-2}
9	C_{10} trihydroxy-nitrate	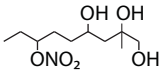	1.56×10^{-1}	2.74×10^{-2}	10	3	1	57	0.75	1.30×10^{-1}
								88	0.36	1.51×10^{-1}
								88	0.37	1.48×10^{-1}
								88	0.32	1.95×10^{-1}
10	C_{11} dihydroxy-nitrate	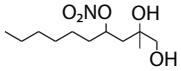	2.36×10^{-2}	8.78×10^{-3}	11	2	1	82	0.86	3.03×10^{-2}
								103	0.84	1.52×10^{-2}
								177	0.27	3.21×10^{-2}
								177	0.37	1.69×10^{-2}
11	C_{11} trihydroxy-nitrate	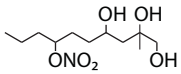	1.67×10^{-1}	1.01×10^{-2}	11	3	1	57	0.66	1.70×10^{-1}
								88	0.35	1.61×10^{-1}
								88	0.36	1.57×10^{-1}
								88	0.33	1.80×10^{-1}
12	C_{12} dihydroxy-nitrate	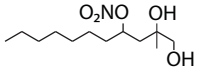	1.75×10^{-2}	8.67×10^{-3}	12	2	1	177	0.29	2.88×10^{-2}
								222	0.37	7.68×10^{-3}
								222	0.27	1.76×10^{-2}
								223	0.28	1.60×10^{-2}
13	C_{12} trihydroxy-nitrate	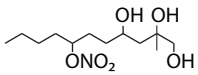	1.77×10^{-1}	6.03×10^{-2}	12	3	1	82	0.43	1.32×10^{-1}
								103	0.33	1.18×10^{-1}
								103	0.23	2.29×10^{-1}
								103	0.23	2.29×10^{-1}
14	C_{13} β-hydroxy-nitrate	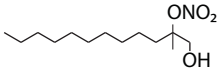	2.66×10^{-3}	1.55×10^{-3}	13	1	1	222	0.57	1.95×10^{-3}
								302	0.44	1.15×10^{-3}
								302	0.35	2.78×10^{-3}
								302	0.29	4.75×10^{-3}
15	C_{13} dihydroxy-nitrate	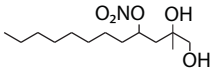	2.75×10^{-2}	2.45×10^{-3}	13	2	1	223	0.21	2.67×10^{-2}
								222	0.23	2.44×10^{-2}
								222	0.20	2.92×10^{-2}
								222	0.20	2.97×10^{-2}

continued ...

Table S2. continued.

Molecule Number	Name	Product structure	κ [-]	stdev [-]	C	OH	ONO_2	D_d [nm]	s_c [%]	κ [-]
16	C_{13} trihydroxy-nitrate	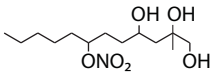	1.04×10^{-1}	3.05×10^{-2}	13	3	1	140	0.24	8.34×10^{-2}
								111	0.32	9.49×10^{-2}
								111	0.34	8.72×10^{-2}
								111	0.26	1.49×10^{-1}
17	C_{14} β-hydroxy-nitrate	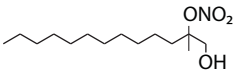	4.89×10^{-5}	7.78×10^{-5}	14	1	1	223	0.98	$< 1\times10^{-5}$
								302	0.82	$< 1\times10^{-5}$
								302	0.85	$< 1\times10^{-5}$
								302	0.58	1.66×10^{-4}
18	C_{14} dihydroxy-nitrate	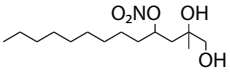	2.61×10^{-2}	1.66×10^{-3}	14	2	1	222	0.21	2.70×10^{-2}
								222	0.23	2.41×10^{-2}
								222	0.22	2.54×10^{-2}
								223	0.21	2.79×10^{-2}
19	C_{14} trihydroxy-nitrate	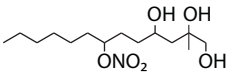	1.01×10^{-1}	2.75×10^{-2}	14	3	1	140	0.27	6.97×10^{-2}
								111	0.33	8.97×10^{-2}
								111	0.29	1.14×10^{-1}
								111	0.27	1.32×10^{-1}
20	C_{15} β-hydroxy-nitrate	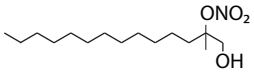	8.35×10^{-4}	1.63×10^{-2}	15	1	1	223	1.11	$< 1\times10^{-5}$
								302	0.70	$< 1\times10^{-5}$
								302	0.63	4.67×10^{-5}
								302	0.33	3.28×10^{-3}
21	C_{15} dihydroxy-nitrate	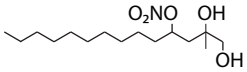	2.17×10^{-2}	1.81×10^{-3}	15	2	1	223	0.24	2.04×10^{-2}
								223	0.24	1.99×10^{-2}
								223	0.23	2.32×10^{-2}
								223	0.23	2.34×10^{-2}
22	C_{15} trihydroxy-nitrate	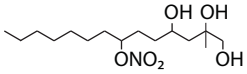	8.12×10^{-2}	2.42×10^{-2}	15	3	1	140	0.27	6.55×10^{-2}
								111	0.39	6.56×10^{-2}
								111	0.36	7.70×10^{-2}
								111	0.29	1.17×10^{-1}
23	C_{14} dinitrate	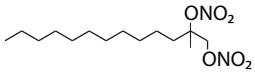	3.55×10^{-3}	6.65×10^{-3}	14	0	2	264	0.23	1.35×10^{-2}
								332	0.74	$< 1\times10^{-5}$
								223	0.70	6.69×10^{-4}
								264	1.03	$< 1\times10^{-5}$
24	C_{14} trinitrate	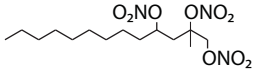	2.92×10^{-4}	3.07×10^{-4}	14	0	3	264	0.82	$< 1\times10^{-5}$
								332	0.46	4.72×10^{-4}
								223	0.70	6.31×10^{-4}
								199	0.97	5.58×10^{-5}
25	C_{14} tetranitrate	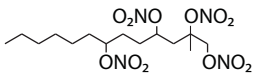	1.17×10^{-3}	4.84×10^{-4}	14	0	4	264	0.58	5.86×10^{-4}
								332	0.37	1.54×10^{-3}
								222	0.60	1.60×10^{-3}
								199	0.75	9.68×10^{-4}

Table S3. Averaged κ values and standard deviation of κ for hydroperoxides generated by gas phase ozonolysis of 1-alkenes in the presence of excess methanol or propanol.[7] CCN analysis was performed by stepping diameter at constant supersaturation.[11] Column 2 contains the reactant 1-alkene (x) and alcohol (y) carbon chain lengths, column 6 is the main product carbon number, columns 7–8 are the number of carbons, hydroperoxide-ether (-C(OOH)-O-) and methylene (-CH_2-) groups per product molecule, and columns 9–11 are the data from different CCN instrument supersaturations. Each Molecule Number corresponds to a separate chamber experiment.

Molecule Number	1-Alkene, Alcohol	Main product	κ [-]	stdev [-]	C	C(OOH) -O-	CH_2	D_d [nm]	s_c [%]	κ [-]
26	7,3	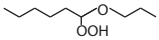	1.07×10^{-1}		9	1	6	90	0.42	1.07×10^{-1}
27	9,1	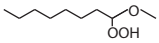	6.26×10^{-2}	5.90×10^{-3}	9	1	6	105	0.42	6.68×10^{-2}
								211	0.16	5.85×10^{-2}
								76	0.63	7.77×10^{-2}
28	8,3	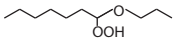	7.61×10^{-2}	9.82×10^{-2}	10	1	7	97	0.42	8.50×10^{-2}
								203	0.16	6.56×10^{-2}
29	10,1	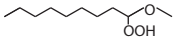	3.37×10^{-2}		10	1	7	131	0.16	3.37×10^{-2}
30	10,1	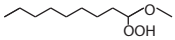	2.96×10^{-2}		10	1	7	136	0.42	2.96×10^{-2}
31	9,3	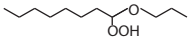	5.00×10^{-2}		11	1	8	115	0.42	5.00×10^{-2}
32	11,1	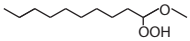	2.52×10^{-2}		11	1	8	280	0.42	2.52×10^{-2}
33	12,1	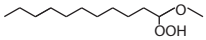	2.35×10^{-2}		12	1	9	147	0.42	2.35×10^{-2}
34	13,1	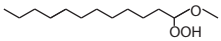	1.39×10^{-2}		13	1	10	175	0.42	1.39×10^{-2}
35	12,3	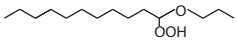	1.90×10^{-2}		14	1	11	157	0.42	1.90×10^{-2}
36	14,1	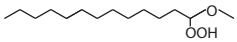	1.33×10^{-2}		14	1	11	177	0.42	1.33×10^{-2}
37	15,1	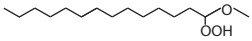	1.67×10^{-2}	1.12×10^{-3}	15	1	12	122	0.63	1.74×10^{-2}
								168	0.42	1.59×10^{-2}
38	14,3	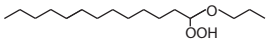	1.46×10^{-2}	4.94×10^{-4}	16	1	13	130	0.63	1.43×10^{-2}
								171	0.42	1.50×10^{-2}
39	16,1	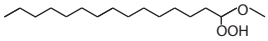	5.43×10^{-3}		16	1	13	139	0.78	5.43×10^{-3}
								91	0.78	2.69×10^{-2}
40	17,1	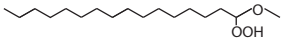	1.89×10^{-2}	7.39×10^{-3}	17	1	14	122	0.63	1.74×10^{-2}
								180	0.42	1.24×10^{-2}

Table S4. CCN experiments of selected alkenes reacted with NO_3 radicals. These reactions produce complex mixtures of molecules with nitrate, hydroxyl and carbonyl functional groups.[12] CCN analysis was performed by stepping diameter at constant supersaturation.[11]

Precursor alkene	Experiment	D_d [nm]	s_c [%]	κ [-]
	#1	> 400	0.78	< 0[§]
1-heptene	#2	> 400	0.78	< 0
	#3	287	0.42	1.89×10^{-3}
1-decene	#1	> 400	0.78	< 0
1-tetradecene	#1	> 400	0.78	< 0
2-methyltridecene	#1	> 400	0.78	< 0
cyclooctene	#1	144	0.42	2.53×10^{-2}
cyclodecene	#1	> 400	0.78	< 0
cyclododecene	#1	> 400	0.78	< 0
α-pinene	#1	> 400	0.78	< 0

[§]No activation was observed at D_d < 400 nm. The CCN activity in s_c-D_d space corresponds to a state less hygroscopic than the insoluble but wetting limit described by $\kappa = 0$.

Table S5. Slopes from linear best fits to the κ values as a function of changing functional groups. Rows 1 and 2 correspond to Figure 2.

Slope	**-OH**	**-C(=O)OH**	**-C(OOH)-O-**	**-ONO$_2$**	**-CH$_2$-**
$d\log_{10}(\kappa)/dn$	1.13	0.71	0.47	-0.24	-0.10
$d\log_{10}(\kappa)/d(O:C)$	10.68	4.99	2.19	-3.37	5.40
$d\ln(\kappa)/dn$	2.60	1.64	1.08	-0.55	-0.24
$d\ln(\kappa)/d(O:C)$	19.03	11.50	5.04	-2.58	12.44

Author Contributions

All authors contributed to conducting the measurements and interpreting the data. MDP, PJZ and SMK designed the study. SRS and MDP wrote the manuscript. All authors have given approval to the final version of the manuscript.

Funding Sources

This research was funded by the Department of Energy, Office of Biological and Environmental Sciences under grant DE-SC0006633.

Acknowledgements

We thank April Ranney for her help with synthesizing some of the compounds. We thank Mary Gilles for discussion of the results.

References

(1) Jimenez, J. L.; Canagaratna, M. R.; Donahue, N. M.; Prévôt, A. S. H.; Zhang, Q.; Kroll, J. H.; DeCarlo, P. F.; Allan, J. D.; Coe, H.; Ng, N. L.; Aiken, A. C.; Docherty, K. S.; Ulbrich, I. M.; Grieshop, A. P.; Robinson, A. L.; Duplissy, J.; Smith, J. D.; Wilson, K. R.; Lanz, V. A.; Hueglin, C.; Sun, Y. L.; Tian, J.; Laaksonen, A.; Raatikainen, T.; Rautiainen, J.; Vaattovaara, P.; Ehn, M.; Kulmala, M.; Tomlinson, J. M.; Collins, D. R.; Cubison, M. J.; Dunlea, E. J.; Huffman, J. A.; Onasch, T. B.; Alfarra, M. R.; Williams, P. I.; Bower, K.; Kondo, Y.; Schneider, J.; Drewnick, F.; Borrmann, S.; Weimer, S.; Demerjian, K.; Salcedo, D.; Cottrell, L.; Griffin, R.; Takami, A.; Miyoshi, T.; Hatakeyama, S.; Shimono, A.; Sun, J. Y.; Zhang, Y. M.; Dzepina, K.; Kimmel, J. R.; Sueper, D.; Jayne, J. T.; Herndon, S. C.; Trimborn, A. M.; Williams, L. R.; Wood, E. C.; Middlebrook, A. M.; Kolb, C. E.; Baltensperger, U.; Worsnop, D. R. Evolution of organic aerosols in the atmosphere. *Science* **2009**, *326*(5959), 1525-1529; DOI 10.1126/science.1180353.

(2) Petters, M. D.; Kreidenweis, S. M.; Prenni, A. J.; Sullivan, R. C.; Carrico, C. M.; Koehler, K. A.; Ziemann, P. J. Role of molecular size in cloud droplet activation. *Geophys. Res. Lett.* **2009**, *36*(22), L22801; DOI 10.1029/2009GL040131.

(3) Chang, R. Y. -W.; Slowik, J. G.; Shantz, N. C.; Vlasenko, A.; Liggio, J.; Sjostedt, S. J.; Leaitch, W. R.; Abbatt, J. P. D. The hygroscopicity parameter (κ) of ambient organic aerosol at a field site subject to biogenic and anthropogenic influences: relationship to degree of aerosol oxidation. *Atmos. Chem. Phys.* **2010**, *10*(11), 5047-5064; DOI 10.5194/acp-10-5047-2010.

(4) Farmer, D. K.; Matsunaga, A.; Docherty, K. S.; Surratt, J. D.; Seinfeld, J. H.; Ziemann, P. J.; Jimenez, J. L. Response of an aerosol mass spectrometer to organonitrates and organosulfates and implications for atmospheric chemistry. *Proc. Natl. Acad. Sci. U. S. A.* **2010**, *107*(15), 6670-6675; DOI 10.1073/pnas.0912340107.

(5) Bailey, P. S. The reactions of ozone with organic compounds. *Chem. Rev.* **1958**, *58*(5), 925-1010; DOI 10.1021/cr50023a005.

(6) Tobias, H. J.; Ziemann, P. J. Thermal desorption mass spectrometric analysis of organic aerosol formed from reactions of 1-tetradecene and O_3 in the presence of alcohols and carboxylic acids. *Environ. Sci. Technol.* **2000**, *34*(11), 2105-2115; DOI 10.1021/es9907156.

(7) Tobias, H. J.; Ziemann, P. J. Kinetics of the gas-phase reactions of alcohols, aldehydes, carboxylic acids, and water with the C13 stabilized Criegee intermediate formed from ozonolysis of 1-tetradecene. *J. Phys. Chem. A* **2001**, *105*(25), 6129-6135; DOI 10.1021/jp004631r.

(8) Suda, S. R.; Petters, M. D.; Matsunaga, A.; Sullivan, R. C.; Ziemann, P. J.; Kreidenweis, S. M. Hygroscopicity frequency distributions of secondary organic aerosols. *J. Geophys. Res.* **2012**, *117*, D04207; DOI 10.1029/2011JD016823.

(9) Matsunaga, A.; Ziemann, P. J. Yields of β-hydroxynitrates, dihydroxynitrates, and trihydroxynitrates formed from OH radical-initiated reactions of 2-methyl-1-alkenes. *Proc. Natl. Acad. Sci. U. S. A.* **2010**, *107*(15), 6664-6669; DOI 10.1073/pnas.0910585107.

(10) Kames, J.; Schurath, U.; Flocke, F.; Volz-Thomas, A. Preparation of organic nitrates from alcohols and N_2O_5 for species identification in atmospheric samples. *J. Atmos. Chem.* **1993**, *16*(4), 349-359; DOI 10.1007/BF01032630.

(11) Petters, M. D.; Carrico, C. M.; Kreidenweis, S. M.; Prenni, A. J.; DeMott, P. J.; Collett, J. L., Jr.; Moosmüller, H. Cloud condensation nucleation activity of biomass burning aerosol. *J. Geophys. Res.* **2009**, *114*, D22205; DOI 10.1029/2009JD012353.

(12) Gong, H.; Matsunaga, A.; Ziemann, P. J. Products and mechanism of secondary organic aerosol formation from reactions of linear alkenes with NO_3 radicals. *J. Phys. Chem. A* **2005**, *109*(19), 4312-4324; DOI 10.1021/jp058024l.